

# Porous indium doped TiO<sub>2</sub> using CTAB as template in a sol-gel process

DECHANG HAN, YUXUAN LIU, WENJIE ZHANG\*

*School of Environmental and Chemical Engineering, Shenyang Ligong University, Shenyang 110159, China*

Cetyltrimethylammonium bromide (CTAB) was used as the template in a sol-gel process to synthesize porous indium doped TiO<sub>2</sub> photocatalyst. TiO<sub>2</sub> is in the anatase phase in both 3%In-TiO<sub>2</sub> and the porous 3%In-TiO<sub>2</sub>(C). The average crystallite sizes of pure TiO<sub>2</sub>, 3%In-TiO<sub>2</sub> and 3%In-TiO<sub>2</sub>(C) samples are 23.9, 13.2 and 15.5 nm, respectively. The pore volume obviously increases after the addition of CTAB. BET surface area of the 3%In-TiO<sub>2</sub>(C) samples are much larger than that of 3%In-TiO<sub>2</sub> when CTAB concentration changes from 0.08 mol/L to 0.2 mol/L. The optimal photocatalytic activity is achieved on the 3%In-TiO<sub>2</sub>(C) sample using 0.12 mol/L CTAB.

(Received March 17, 2016; accepted February 10, 2017)

*Keywords:* TiO<sub>2</sub>, Indium, Photocatalysis, Cetyltrimethylammonium bromide

## 1. Introduction

TiO<sub>2</sub> is an important photocatalyst on degradation of organic pollutants, and it has been studied for decades [1]. The major defects in using TiO<sub>2</sub> are the large band gap and high recombination rate of this potential material [2,3]. As a modification method, metal ion doping in TiO<sub>2</sub> is attempted to extend the lifetime of photogenerated charge carriers by retarding recombination of electrons and holes [4]. Therefore, photocatalytic activity of TiO<sub>2</sub> based material is improved [5,6]. Among the various elements used for this purpose, indium as a dopant in TiO<sub>2</sub> photocatalyst was reported in the recent years [7-10].

Porous material is considered to have high adsorption capacity and photocatalytic activity due to the large surface area and highly ordered porous structure [11]. Porous TiO<sub>2</sub> based materials usually have great photocatalytic efficiency [12-14]. Cetyltrimethylammonium bromide (CTAB) is a surfactant and is used as template agent in synthesizing porous structured materials [15-18].

It would be interesting to use CTAB in synthesizing porous indium doped TiO<sub>2</sub> material. In this work, porous indium doped TiO<sub>2</sub> was prepared through a sol-gel route by the addition of CTAB. The obtained materials were characterized by XRD, SEM and N<sub>2</sub> adsorption-desorption measurements. Methyl orange was used as the pollutant to measure the adsorption capacity and photocatalytic activity of the porous indium doped TiO<sub>2</sub>.

## 2. Experimental

### 2.1. Synthesis of the materials

CTAB was used as the template to prepare indium

doped porous TiO<sub>2</sub> through a sol-gel route. Different amount of CTAB and 0.0675 g In(NO<sub>3</sub>)<sub>3</sub>·4.5H<sub>2</sub>O were dissolved in 8 mL anhydrous ethanol, and then 2 mL tetrabutyl titanate and 0.1 mL concentrated hydrochloric acid were added. 0.9 mL distilled water and 4 mL anhydrous ethanol were mixed to form another solution. The two solutions were slowly mixed together to form a transparent precursor. A gel formed after 1 h under continuous stirring. After aging at ambient temperature for 24 h, the gel was subsequently dried at 80 °C for 8 h. The solid was ground and calcinated at 500 °C for 3 h. The products were ground again and marked as 3%In-TiO<sub>2</sub>(C), where C represents the concentration of CTAB in the precursor. In this work, CTAB concentration is 0.12 mol/L if not indicated.  $n(\text{In})/n(\text{Ti})$  is 0.03 in all the samples.

### 2.2. Characterization of the materials

X-ray diffraction measurement of the material was studied by a Rigaku D/Max-rB diffractometer using Cu K $\alpha$  radiation. The XRD calculation of crystallite size was based on the Scherrer formula. The morphology of the material was studied by scanning electron microscopy (SEM. Hitachi, S-3400N). A thin layer of gold was coated on the sample to avoid charging. The specific surface area was determined by the multipoint BET method using the adsorption data in the relative pressure ( $P/P_0$ ) range between 0.05-0.25. The desorption isotherm was studied to determine pore size distribution using the BJH (Barrett-Joyner-Halenda) method.

### 2.3. Photocatalytic activity

Methyl orange (MO) decolorization was used to

measure the activity of the 3%In-TiO<sub>2</sub>(C) photocatalyst. 15 mg photocatalyst was mixed with 50 mL 10 mg/L methyl orange aqueous solution in a 100 mL quartz beaker. The suspension was stirred for 60 min to reach adsorption-desorption equilibrium. Subsequently, a 20 W UV-light lamp, irradiating at 253.7 nm, was used as the UV light source to excite the photocatalytic reaction. The average irradiation intensity striking the solution was 1300  $\mu\text{W}/\text{cm}^2$ . The MO solution could not be decolorized under irradiation without the photocatalyst. After 30 min irradiation, 5 mL of the suspension was filtrated by a millipore filter (pore size 0.22  $\mu\text{m}$ ) to measure the change of MO concentration.

### 3. Results and discussion

Fig. 1 shows XRD patterns of pure TiO<sub>2</sub>, 3%In-TiO<sub>2</sub> and 3%In-TiO<sub>2</sub>(C). The diffraction peaks of all the samples are in accordance to the diffraction peaks of anatase phase TiO<sub>2</sub> (ICDD 03-065-5714). Other phases of TiO<sub>2</sub> and indium-containing substances are not observed in the spectra. The doping of indium results in an apparent shrinking of the diffraction intensity, while the addition of CTAB template has very minor influence on anatase TiO<sub>2</sub> formation. Scherrer formula is used to calculate the crystallite size of the anatase TiO<sub>2</sub> on the (101) plane. The average crystallite sizes of pure TiO<sub>2</sub>, 3%In-TiO<sub>2</sub> and 3%In-TiO<sub>2</sub>(C) samples are 23.9, 13.2 and 15.5 nm, respectively. Crystallite size of TiO<sub>2</sub> becomes much smaller after doping of indium. Furthermore, the crystallite size does not change much after the addition of CTAB. Lattice parameters of pure TiO<sub>2</sub>, 3%In-TiO<sub>2</sub> and 3%In-TiO<sub>2</sub>(C) are listed in Table 1. The doping of indium leads to increments of lattice parameters and cell volume due to the substitution of Ti<sup>4+</sup> ion by In<sup>3+</sup> ion in the TiO<sub>2</sub> skeleton. The addition of CTAB does not put apparent influence on the lattice parameters of anatase TiO<sub>2</sub>.

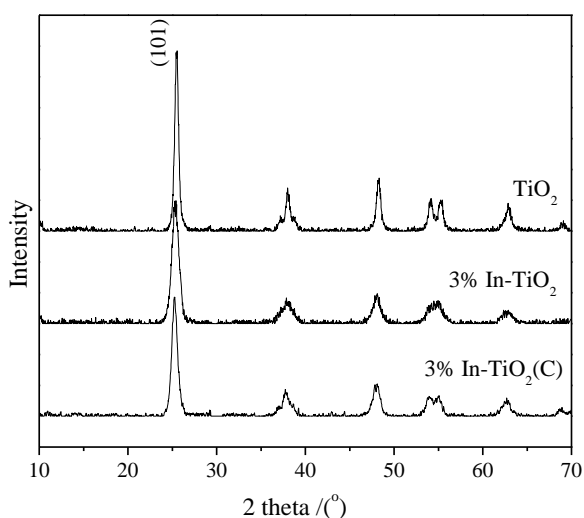


Fig. 1. XRD patterns of pure TiO<sub>2</sub>, 3%In-TiO<sub>2</sub> and 3%In-TiO<sub>2</sub>(C).

Table 1. Lattice parameters of TiO<sub>2</sub> and 3%In-TiO<sub>2</sub>(C)

Sample	$a(=b) / 10^{-1} \text{ nm}$	$c / 10^{-1} \text{ nm}$	$V / 10^{-3} \text{ nm}^3$
TiO <sub>2</sub>	3.7831	9.4756	135.78
3%In-TiO <sub>2</sub>	3.7922	9.4793	136.35
3%In-TiO <sub>2</sub> (C)	3.7939	9.4798	136.47

Fig. 2 shows the SEM images of pure TiO<sub>2</sub>, 3%In-TiO<sub>2</sub> and 3%In-TiO<sub>2</sub>(C). Small particles scatter among the large particles in the samples. The morphologies of the samples are almost the same. Large particles in the size as large as 3-4  $\mu\text{m}$  are surrounded by small particles in the size below 100 nm. The small particles may be produced during grinding. Neither the doping of indium nor the addition of CTAB makes noticeable influence on the surface morphology of the materials.

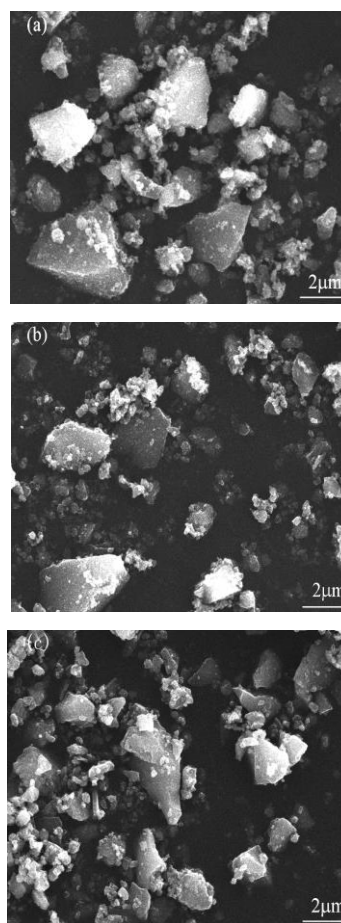


Fig. 2. SEM images of (a) TiO<sub>2</sub>, (b) 3%In-TiO<sub>2</sub> and (c) 3%In-TiO<sub>2</sub>(C)

N<sub>2</sub> desorption isotherms of pure TiO<sub>2</sub>, 3%In-TiO<sub>2</sub> and 3%In-TiO<sub>2</sub>(C) are shown in Fig. 3. The adsorbed volume of N<sub>2</sub> on the surface of the materials depends on the partial pressure of N<sub>2</sub>. The adsorbed amount of N<sub>2</sub> is not large at N<sub>2</sub> partial pressure below 0.6. The adsorbed N<sub>2</sub> volume drastically increases at higher relative pressure, partly due to capillary condensation of N<sub>2</sub> in the micropores of the samples. The 3%In-TiO<sub>2</sub>(C) can apparently adsorb more N<sub>2</sub> than the other materials without using CTAB. The addition of CTAB might result in porous structure to enhance the adsorption capacity of the material.

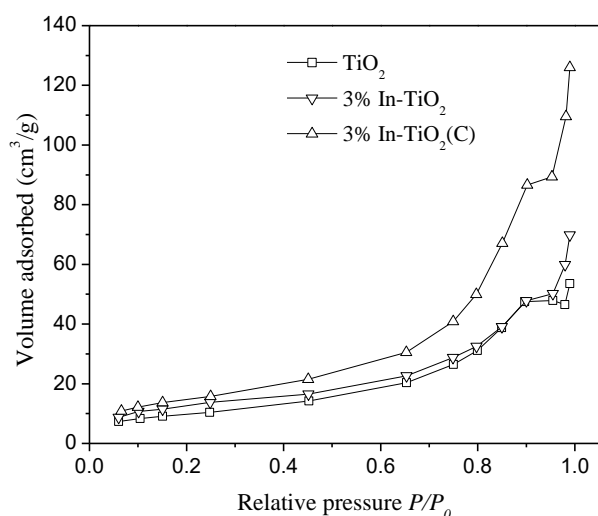


Fig. 3. N<sub>2</sub> desorption isotherms of pure TiO<sub>2</sub>, 3%In-TiO<sub>2</sub> and 3%In-TiO<sub>2</sub>(C)

Fig. 4 shows BJH pore size distributions of pure TiO<sub>2</sub>, 3%In-TiO<sub>2</sub> and 3%In-TiO<sub>2</sub>(C). The samples contain a certain amount of mesopores in the size between 2 and 20 nm. The overall pore volume obviously increases after the addition of CTAB, although pore size distribution range does not apparently change at the same time. The increase of mesopores in the 3%In-TiO<sub>2</sub>(C) sample can be regarded as the result of CTAB template addition. Meanwhile, there are still inter-particle macropores in the materials coming from particles aggregation.

Materials with small particle size and porous structure usually have large specific surface area. Adsorption capacity of the materials depends on their surface area. The BET specific surface areas of pure TiO<sub>2</sub> and 3%In-TiO<sub>2</sub> are 36.6 and 39.1 m<sup>2</sup>/g. Indium doping has very minor influence on the surface area. An apparent increase of specific surface area is found after addition of CTAB, although CTAB concentration has slight effect on surface area of the samples. BET surface area of the 3%In-TiO<sub>2</sub>(C) samples are 57.0, 59.4 and 53.2 m<sup>2</sup>/g when CTAB concentration changes from 0.08 mol/L to 0.2 mol/L.

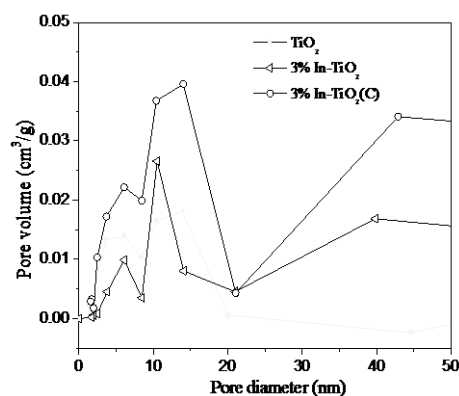


Fig. 4. BJH pore size distribution of pure TiO<sub>2</sub>, 3%In-TiO<sub>2</sub> and 3%In-TiO<sub>2</sub>(C)

Fig. 5 shows adsorption and photocatalytic degradation of methyl orange on 3%In-TiO<sub>2</sub>(C) using different concentration of CTAB. Fig. 5(a) represents decoloration efficiency as a factor of CTAB concentration. Adsorption of methyl orange slightly varies with the change in CTAB concentration. When CTAB concentrations are 0.08 and 0.12 mol/L in the precursor, the samples possess enhanced photocatalytic activity as compared to the sample without using CTAB. The optimal photocatalytic activity is achieved on the 3%In-TiO<sub>2</sub>(C) sample using 0.12 mol/L CTAB.

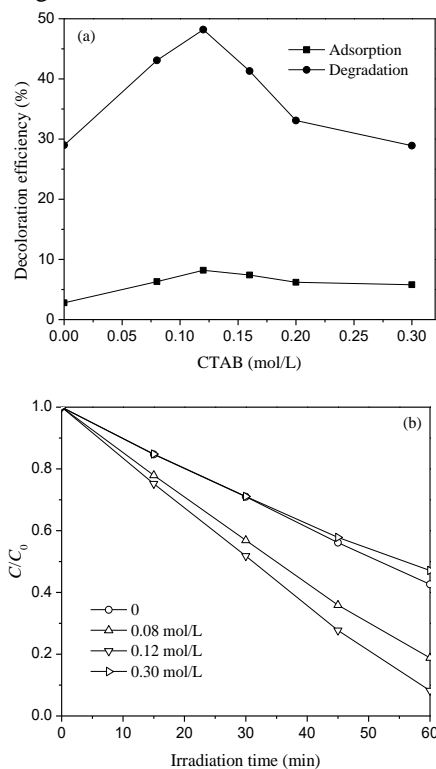


Fig. 5. Adsorption and photocatalytic degradation of methyl orange on 3%In-TiO<sub>2</sub>(C) using different concentration of CTAB. (a) Decoloration efficiency as a factor of CTAB concentration, (b) Photocatalytic degradation with prolonged irradiation time

Photocatalytic degradation of methyl orange with prolonged irradiation time is shown in Fig. 5(b). Decoloration efficiency of the dye increases with extending reacting time on all the samples without apparent losing of photocatalytic activity. Photocatalytic degradation efficiency is 91.8% after 60 min of irradiation on the 3%In-TiO<sub>2</sub>(C) sample using 0.12 mol/L CTAB. The degradation efficiency is nearly 35% higher than the sample without using CTAB. Excessive addition of CTAB is not favored to further enhancing the activity.

#### 4. Conclusions

Porous indium doped TiO<sub>2</sub> materials were synthesized by sol-gel method to study the influence of CTAB template addition on the properties of 3%In-TiO<sub>2</sub>(C). TiO<sub>2</sub> is in the anatase phase in both 3%In-TiO<sub>2</sub> and the porous 3%In-TiO<sub>2</sub>(C). An apparent increase of specific surface area is obtained after using CTAB, although CTAB concentration has slight effect on the surface area of the samples. The porous 3%In-TiO<sub>2</sub>(C) samples possess enhanced photocatalytic activity as compared to 3%In-TiO<sub>2</sub>.

#### Acknowledgment

This work was supported by the Natural Science Foundation of Liaoning Province (No. 2015020186).

#### References

- [1] D. Chatterjee, S. Dasgupta, J. Photochem. Photobiol. **C6**, 186 (2005).
- [2] M. Bellardita, A. D. Paola, B. Megna, L. Palmisano, Appl. Catal. B: Environ. **201**, 150 (2017).
- [3] G. Plantard, T. Janin, V. Goetz, S. Brosillon, Appl. Catal. B: Environ. **115-116**, 38 (2012).
- [4] A. V. Rosario, E. C. Pereira, Appl. Catal. B: Environ. **144**, 840 (2014).
- [5] J. H. Lim, P. Murugan, N. Lakshminarasimhan, J. Y. Kim, J. S. Lee, S. H. Lee, W. Y. Choi, J. Catal. **310**, 91 (2014).
- [6] W. J. Zhang, T. T. Hu, B. Yang, P. Sun, H. B. He, J. Adv. Oxid. Technol. **16**, 261 (2013).
- [7] W. J. Zhang, Y. X. Liu, X. B. Pei, X. J. Chen, J. Phys. Chem. Solids **104**, 45 (2017).
- [8] E. J. Wang, W. S. Yang, Y. A. Gao, J. Phys. Chem. C **113**, 20912 (2009).
- [9] J. B. Mu, B. Chen, M. Y. Zhang, Z. C. Guo, P. Zhang, Z. Y. Zhang, Appl. Mater. Inter. **4**, 424 (2012).
- [10] W. J. Zhang, C. G. Li, Z. Ma, L. L. Yang, H. B. He, J. Adv. Oxid. Technol. **19**, 119 (2016).
- [11] H. Yoshitake, T. Sugihara, T. Tatsumi, Chem. Mater. **14**, 1023 (2002).
- [12] Q. R. Sheng, S. Yuan, J. L. Zhang, F. Chen, Micropor. Mesopor. Mater. **87**, 177 (2006).
- [13] N. Arconada, A. Dura, S. Suarez, R. Portela, J. M. Coronado, B. Sanchez, Y. Castro, Appl. Catal. B: Environ. **86**, 1 (2009).
- [14] Y. Zhao, X. T. Zhang, Appl. Catal. B: Environ. **83**, 24 (2008).
- [15] C. X. Song, D. B. Wang, Y. H. Xu, Mater. Lett. **65**, 908 (2011).
- [16] Y. Xie, X. J. Zhao, Y. Z. Li, J. Solid State Chem. **181**, 1936 (2008).
- [17] S. Casino, F. D. Lupo, C. Francia, A. Tuel, S. Bodoardo, C. Gerbaldi, J. Alloys Compd. **594**, 114 (2014).
- [18] M. M. Mohamed, M. S. Al-Sharif, Appl. Catal. B: Environ. **142-143**, 432 (2013).

\*Corresponding author: wjzhang@aliyun.com